Bulk viscosity for pion and nucleon thermal fluctuation in the hadron resonance gas model

Sabyasachi Ghosh,[1,2,*] Sandeep Chatterjee,[2,3,†] and Bedangadas Mohanty[2,‡]
[1]*Department of Physics, University of Calcutta, 92, A. P. C. Road, Kolkata - 700009, India*
[2]*School of Physical Sciences, National Institute of Science Education and Research Bhubaneswar, HBNI, Jatni, 752050, India*
[3]*Theoretical Physics Division, Variable Energy Cyclotron Centre, 1/AF, Bidhan Nagar, Kolkata - 700064, India*
(Received 16 July 2016; revised manuscript received 17 September 2016; published 25 October 2016)

We have calculated microscopically bulk viscosity of hadronic matter, where equilibrium thermodynamics for all hadrons in medium are described by the hadron resonance gas (HRG) model. Considering pions and nucleons as abundant medium constituents, we have calculated their thermal widths, which inversely control the strength of bulk viscosities for respective components and represent their in-medium scattering probabilities with other mesonic and baryonic resonances, present in the medium. Our calculations show that bulk viscosity increases with both temperature and baryon chemical potential, whereas viscosity to entropy density ratio decreases with temperature and with baryon chemical potential, the ratio increases first and then decreases. The decreasing nature of the ratio with temperature has been observed in most of the earlier investigations with few exceptions. We find that the temperature dependence of bulk viscosity crucially depends on the structure of the relaxation time. Along the chemical freeze-out line in nucleus-nucleus collisions with increasing collision energy, bulk viscosity as well as the bulk viscosity to entropy density ratio decreases, which also agrees with earlier references. Our results indicate the picture of a strongly coupled hadronic medium.

DOI: 10.1103/PhysRevC.94.045208

I. INTRODUCTION

The extraction of the transport properties of the strongly interacting medium created in heavy ion collision (HIC) experiments is currently a very active topic of research in the HIC community. The methods of relativistic hydrodynamics with minimal viscous correction have been quite successful in describing the time evolution of the hot and dense fireball created in the HIC experiments. These kinds of investigations have also concluded that the shear viscosity (η) to entropy density (s) ratio, η/s, of the medium created in HIC experiments is very close to its quantum lower bound $1/4\pi$ [1]. Similar to η, another transport coefficient is the bulk viscosity, ζ, which is defined as the proportionality constant between the nonzero trace of the viscous stress tensor to the divergence of the fluid velocity, and usually it appears associated with processes accompanied by a change in fluid volume or density. The viscous coefficient ζ has received much less attention than the η in hydrodynamical simulations because its numerical value is assumed to be very small, as it is directly proportional to the trace of the energy-momentum tensor, which generally vanishes for conformally symmetric matter [2]. However, according to lattice quantum chromodynamics (LQCD) calculations [3], the trace of the energy momentum tensor of hot QCD medium might be large near the QCD phase transition, which indicates the possibility of a nonzero and large value of ζ as well as ζ/s near the transition temperature. This indication is confirmed by Refs. [4,5], related with LQCD estimation, where Ref. [5] exposes the possibility of divergence of ζ near the transition temperature. In recent times, different phenomenological investigations [6–18] demonstrated that bulk viscosity can have a non-negligible effect on heavy ion observables, where the values of ζ/s in Ref. [18] is assumed to be quite large.

On the basis of phenomenological importance, microscopic calculations of ζ for quark gluon plasma (QGP) and hadronic matter is of contemporary interest to the HIC community. A list of references are [2,19–38], where Ref. [19] addressed high temperature perturbative QCD calculations of ζ, Refs. [20–25] have gone through Nambu–Jona-Lasinio (NJL) model calculations of ζ, and Refs. [26–28] provided the discussions on linear sigma model (LSM) estimation of ζ. These effective QCD model calculations [20–28] cover both QGP and hadronic phases while hadronic-model calculations of Refs. [32–37] are restricted within hadronic phase only. The present work addresses the estimation of ζ in the hadronic phase only. At vanishing baryonic chemical potential, most of the microscopic calculations predict that $\zeta(T)$ increases but $\zeta/s(T)$ decreases in the hadronic temperature domain. However, few exceptions are there depending on different scenario. For example, Ref. [28] showed that the decreasing function of $\zeta/s(T)$ is transformed to an increasing function in the hadronic temperature domain, when its medium constituents sigma meson becomes heavier. Similar observation is also made in Ref. [27] depending on the different nature of phase transition as well as methodological differences of LSM calculations. In the hadronic temperature domain, a decreasing nature of $\zeta(T)$ is observed in Ref. [20] while Ref. [33] estimated increasing $\zeta/s(T)$. Thus the nature of $\zeta(T)$ and $\zeta/s(T)$ are not settled issues. Again, the numerical strength of ζ and ζ/s from different model calculations exhibit a large band—$\zeta \sim 10^{-5}$ GeV^3 [32] to 10^{-2} GeV^3 [20] or $\zeta/s \sim 10^{-3}$ [32] to 10^0 [20]. These uncertainties in nature as well as numerical values of $\zeta(T)$ from the earlier investigations demand further research on these kind of microscopic calculations. Owing

*sabyaphy@gmail.com
†sandeepc@niser.ac.in
‡bedanga@niser.ac.in

to that motivation, we have gone through a microscopic calculations of ζ and ζ/s, where the equilibrium hadronic matter is emulated by the standard HRG model and the nonequilibrium picture of medium constituents is introduced via quantum fluctuation of pion and nucleon in medium.

Among the earlier HRG calculations of ζ [33–36], Refs. [33,36] have taken the Kubo-type expression of ζ in the QCD sum rule approach [2,5], while Ref. [34] has taken the expression of ζ, based on the relaxation time approximation, which is adopted in the present work. The thermal width, which is inversely equal to the relaxation time, plays an important role to determine the numerical strength of ζ. Reference [34] has considered constant thermal width or relaxation time and a constant hard sphere cross section. Hence, the dependence on the medium temperature and baryon chemical potential enters only through the phase space of the medium constituents. In contrast to this approach, in the present work we have performed an explicit calculation of thermal width based on an underlying interaction Lagrangian. This calls for a nontrivial dependence on the momentum of medium constituents and on the medium temperature and baryon chemical potential. Assuming pions and nucleons as most abundant constituents of medium, we have calculated their thermal width, which comes from their in-medium scattering with different possible mesonic and baryonic resonances.

The article is written as follows. The main formalism for the thermal width calculations of pion and nucleon are explicitly described in Sec. II. We provide a brief description of the HRG model that models the equilibrium part. Next, the numerical results are discussed in Sec. III and lastly, our investigations have been summarized and concluded in Sec. IV.

II. FORMALISM

The HRG is an ideal gas of hadrons and resonances taken from the Particle Data Book [39]. Here we consider all those resonances with masses up to 2 GeV. The recent LQCD data at zero baryon chemical potential (μ_B) show that for temperatures up to the crossover region (150–160 MeV), HRG provides a reasonably good description of the LQCD thermodynamics [40–42]. All thermodynamic quantities of the HRG can be computed from the logarithm of total partition function

$$\ln Z_{HRG}(T,\mu_B,\mu_Q,\mu_S) = \sum_i \ln Z_s^i(T,\mu_B,\mu_Q,\mu_S), \quad (1)$$

where

$$\ln Z_s^i = \frac{g_i}{2\pi^2} V T^3 \sum_{n=1}^{\infty} \frac{(\mp 1)^{(n+1)}}{n^4} \left(\frac{n m_i}{T}\right)^2 K_2\left(\frac{n m_i}{T}\right) e^{n\beta\mu_i} \quad (2)$$

is the single particle partition function of the ith hadron. In Eq. (2), g_i is the degeneracy factor of ith particle with mass m_i, V is volume of the medium, and $K_2(\cdots)$ is the modified Bessel function. Under the condition of complete chemical equilibrium, all the hadron chemical potentials can be expressed in terms of only three chemical potentials corresponding to the QCD conserved charges

$$\mu_i = B_i\mu_{Bi} + Q_i\mu_{Q_i} + S_i\mu_{S_i}, \quad (3)$$

where B_i, Q_i, and S_i are the baryon number, electric charge and strangeness of the ith hadron. It is straightforward to compute other thermodynamic quantities from $Z_{\rm HRG}$, such as pressure (P), energy density (ϵ), entropy density (s):

$$P = -\frac{T}{V}\ln Z_{\rm HRG}, \quad (4)$$

$$\epsilon = \frac{1}{V}\left\{T^2\frac{\partial \ln Z_{\rm HRG}}{\partial T} + \sum_i \mu_i T \frac{\partial \ln Z_{\rm HRG}}{\partial \mu_i}\right\}, \quad (5)$$

$$s = \frac{1}{T}\left\{\epsilon + P - \frac{1}{V}\sum_i \mu_i T \frac{\partial \ln Z_{\rm HRG}}{\partial \mu_i}\right\}. \quad (6)$$

Square of the speed of sound for constant baryon density (n_B), entropy density (s), and entropy per baryon ($\sigma = s/n_B$) are, respectively, defined as

$$v^2_{n,s,\sigma} = \left(\frac{\partial P}{\partial \epsilon}\right)_{n_B,s,\sigma}. \quad (7)$$

Among them, sound wave at constant σ only propagates in the expanding nuclear medium, produced in heavy ion collisions, because σ is conserved during ideal hydrodynamical expansion of the medium and therefore, it must be fixed during the estimation of thermodynamical variations from the equilibrium [43].

From the relaxation time approximation (RTA) of kinetic theory approach [28,31,43] or from the one-loop expression of diagrammatic approach based on Kubo formula [37], we can get standard expressions of bulk viscosity coefficient for pion and nucleon components [43]

$$\zeta_\pi = \left(\frac{g_\pi}{T}\right)\int \frac{d^3\vec{k}}{(2\pi)^3}\frac{n_\pi[1+n_\pi]}{\omega_\pi^2\,\Gamma_\pi}\left\{\left(\frac{1}{3}-v_n^2\right)\vec{k}^2 - v_n^2 m_\pi^2\right\}^2 \quad (8)$$

and

$$\begin{aligned}\zeta_N = \left(\frac{g_N}{T}\right)\int \frac{d^3\vec{k}}{(2\pi)^3}\frac{1}{\omega_N^2\,\Gamma_N}\Bigg[& n_N^+(1-n_N^+)\Bigg\{\frac{\vec{k}^2}{3} + v_n^2 T^2\omega_N\frac{\partial}{\partial T}\left(\frac{\omega_N-\mu_B}{T}\right)_\sigma\Bigg\}^2 + \Bigg\{\frac{\vec{k}^2}{3} + v_n^2 T^2\omega_N\frac{\partial}{\partial T}\left(\frac{\omega_N+\mu_B}{T}\right)_\sigma\Bigg\}^2 n_N^-(1-n_N^-)\Bigg] \\ = \left(\frac{g_N}{T}\right)\int \frac{d^3\vec{k}}{(2\pi)^3}\frac{1}{\omega_N^2\,\Gamma_N}\Bigg[&\Bigg\{\left(\frac{1}{3}-v_n^2\right)\vec{k}^2 - v_n^2 m_N^2 - \omega_N\left(\frac{\partial P}{\partial n_B}\right)_\epsilon\Bigg\}^2 n_N^+(1-n_N^+) + \Bigg\{\left(\frac{1}{3}-v_n^2\right)\vec{k}^2 - v_n^2 m_N^2 + \omega_N\left(\frac{\partial P}{\partial n_B}\right)_\epsilon\Bigg\}^2 n_N^-(1-n_N^-)\Bigg],\end{aligned} \quad (9)$$

where $n_\pi = 1/\{e^{\omega_\pi/T}-1\}$ is the Bose-Einstein (BE) distribution function of pion with energy $\omega_\pi = \{\vec{k}^2+m_\pi^2\}^{1/2}$, $n_N^\pm = 1/\{e^{(\omega_N\mp\mu_B)/T}+1\}$ are the Fermi-Dirac (FD) distribution functions of nucleon and antinucleon, respectively, with energy $\omega_N = \{\vec{k}^2+m_N^2\}^{1/2}$ at finite temperature T and baryon

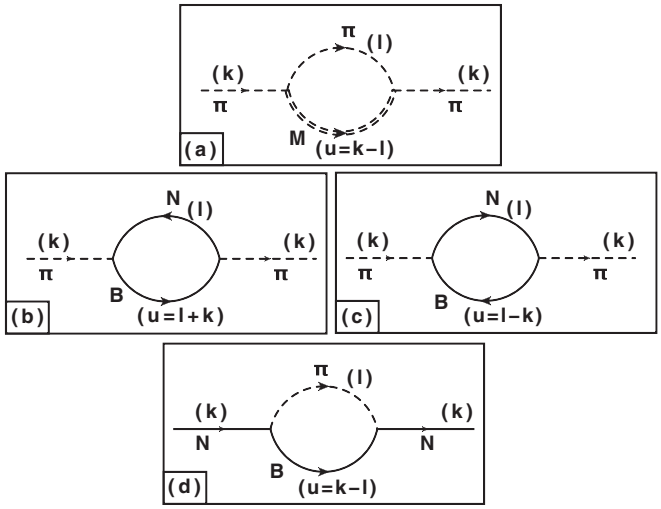

FIG. 1. Pion self-energy diagram with mesonic loops (a) and baryonic loops [(b) and (c) are direct and cross diagrams] and nucleon self-energy diagram (d).

chemical potential μ_B. The degeneracy factors of pion and nucleon components are $g_\pi = 3$ and $g_N = 2 \times 2$, respectively.

Next, let us come to the important quantities Γ_π and Γ_N of Eqs. (8) and (9), which are called thermal widths of pion and nucleon, respectively. During propagation in the medium, pion, and nucleon may go through different on-shell scattering with other mesonic (M) and baryonic (B) resonances, which can be quantified by their different possible self-energy diagrams. From the imaginary part of their self-energy functions, their respective thermal widths Γ_π and Γ_N can be found. Figure 1(a) represents pion self-energy with internal lines of pion (π) and other mesonic resonances (M), which we can shortly call the πM loop. We will take $M = \sigma$ and ρ, as they are dominant resonances of $\pi\pi$ decay channel (within the invariant mass range of 1 GeV). Now, from the retarded self-energy of pion for πM loop $\Pi^R_{\pi(\pi M)}(k)$, the corresponding thermal width $\Gamma_{\pi(\pi M)}$ can be obtained as

$$\Gamma_{\pi(\pi M)} = -\mathrm{Im}\Pi^R_{\pi(\pi M)}(k_0 = \omega_\pi, \vec{k})/m_\pi, \tag{10}$$

where the subscript notation stands for external (outside the bracket) and internal (inside the bracket) particles for Fig. 1(a). Following similar notation, we can define

$$\Gamma_{\pi(NB)} = -\mathrm{Im}\Pi^R_{\pi(NB)}(k_0 = \omega^\pi_k, \vec{k})/m_\pi, \tag{11}$$

where intermediate states of pion self-energy are nucleon N and other baryonic resonance B as shown in Fig. 1(b) along with its cross diagram (c). As a dominant four-star baryons with spin $J_B = 1/2$ and $3/2$, we have taken $B = \Delta(1232)$, $N^*(1440)$, $N^*(1520)$, $N^*(1535)$, $\Delta^*(1600)$, $\Delta^*(1620)$, $N^*(1650)$, $\Delta^*(1700)$, $N^*(1700)$, $N^*(1710)$, and $N^*(1720)$. Adding all these mesonic (πM) and baryonic (NB) loops, the total thermal width of pion Γ_π can be obtained as

$$\Gamma_\pi = \Gamma^M_\pi + \Gamma^B_\pi = \sum_M \Gamma_{\pi(\pi M)} + \sum_B \Gamma_{\pi(NB)}. \tag{12}$$

Similarly, one-loop self-energy of nucleon with pion (π) and baryon (B) intermediate states, which is denoted as $\Sigma^R_{N(\pi B)}$ (retarded part), will be our matter of interest to estimate corresponding nucleon thermal width $\Gamma_{N(\pi B)}$. The diagrammatic anatomy of $\Sigma^R_{N(\pi B)}$ is shown in Fig. 1(d). Here we have taken all the four-star spin $1/2$ and $3/2$ baryons, mentioned above. Hence, summing all the πB loops, we can get our total nucleon thermal width:

$$\Gamma_N = \sum_B \Gamma_{N(\pi B)} = -\sum_B \mathrm{Im}\Sigma^R_{N(\pi B)}(k_0 = \omega_N, \vec{k}). \tag{13}$$

The imaginary part of self-energies, given in Eqs (10), (11), and (13), have been derived with help of standard thermal field theoretical techniques. At first, the expression for $\mathrm{Im}\Pi^R_{\pi(\pi M)}$ is [44]

$$\mathrm{Im}\Pi^R_{\pi(\pi M)}(k_0 = \omega_\pi, \vec{k}) = \int \frac{d^3\vec{l}}{32\pi^2\omega_l\omega_u} L_{\pi\pi M}(k,l)|_{(l_0=-\omega_l, k_0=\omega_k)} (n_l - n_u)\delta(\omega_\pi + \omega_l - \omega_u), \tag{14}$$

where n_l, n_u are BE distribution functions of π, M mesons, respectively, at energies $\omega_l = \{\vec{l}^2 + m^2_\pi\}^{1/2}$ and $\omega_u = \{(\vec{k} - \vec{l})^2 + m^2_M\}^{1/2}$. The vertex factors $L_{\pi(\pi M)}(k,l)$ [44] have been calculated by using the effective Lagrangian density,

$$\mathcal{L}_{\pi\pi M} = g_\rho\, \vec{\rho}_\mu \cdot \vec{\pi} \times \partial^\mu \vec{\pi} + \frac{g_\sigma}{2} m_\sigma \vec{\pi} \cdot \vec{\pi}\, \sigma, \tag{15}$$

where g_ρ and g_σ are, respectively, effective coupling constants of ρ meson field ($\vec{\rho}_\mu$) and σ meson field (σ), which are coupled with the pion field ($\vec{\pi}$).

Next, the direct and cross diagrams of pion self-energy for the NB loop combined are expressed as [46,47]

$$\mathrm{Im}\Pi^R_{\pi(NB)}(k_0 = \omega_\pi, \vec{k}) = \int \frac{d^3\vec{l}}{32\pi^2\omega_l\omega_u} L_{\pi NB}(k,l)|_{(l_0=-\omega_l, k_0=\omega_k)} \{(-n^+_l + n^+_u)\delta(\omega_\pi + \omega_l - \omega_u) + (-n^-_l + n^-_u)\delta(\omega_\pi - \omega_l + \omega_u)\}, \tag{16}$$

where $n^\pm_l$, $n^\pm_u$ are FD distribution functions of N and B ($\pm$ for particle and antiparticle), respectively, at energies $\omega_l = \{\vec{l}^2 + m^2_N\}^{1/2}$ and $\omega_u = \{(\vec{k} \pm \vec{l})^2 + m^2_B\}^{1/2}$ [$\pm$ for diagrams (b) and (c), respectively]. With the help of the effective Lagrangian densities for πNB interactions [45],

$$\mathcal{L}_{\pi NB} = \frac{f}{m_\pi}\overline{\psi}_B\gamma^\mu \begin{Bmatrix} i\gamma^5 \\ \mathbb{1} \end{Bmatrix} \psi_N \partial_\mu \pi + \mathrm{h.c.} \quad \text{for } J^P_B = \frac{1}{2}^\pm, \\ = \frac{f}{m_\pi}\overline{\psi}^\mu_B \begin{Bmatrix} \mathbb{1} \\ i\gamma^5 \end{Bmatrix} \psi_N \partial_\mu \pi + \mathrm{h.c.} \quad \text{for } J^P_B = \frac{3}{2}^\pm, \\ (P \text{ stands for parity of } B) \tag{17}$$

one can deduce the vertex factors $L_{\pi NB}(k,l)$ [46,47]. At last, the expression for $\mathrm{Im}\Pi^R_{N(\pi B)}$ is [48,49]

$$\mathrm{Im}\Pi^R_{N(\pi B)}(k_0 = \omega_\pi, \vec{k}) = \int \frac{d^3\vec{l}}{32\pi^2\omega_l\omega_u} L_{N\pi B}(k,l)|_{(l_0=-\omega_l, k_0=\omega_k)} \times (n_l + n^+_u)\delta(\omega_\pi + \omega_l - \omega_u), \tag{18}$$

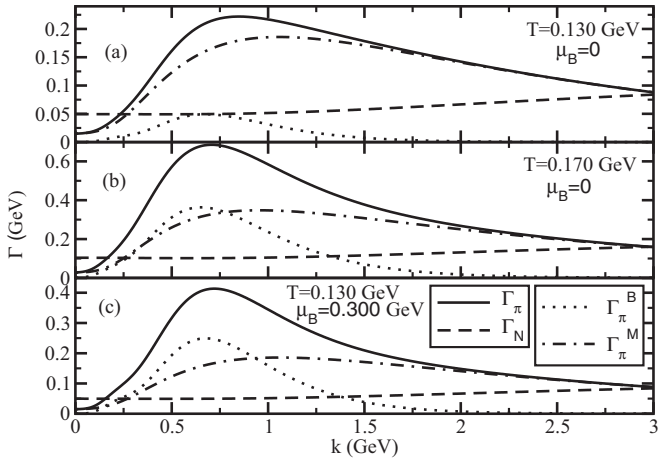

FIG. 2. Momentum dependence of pion thermal width for mesonic (dash-dotted line), baryonic loops (dotted line), and their total (solid line) and nucleon thermal width (dashed line) at three different medium parameters: (a) $(T,\mu_B) = (0.130\ \text{GeV}, 0)$, (b) (0.170 GeV, 0), and (c) (0.130 GeV, 0.300 GeV).

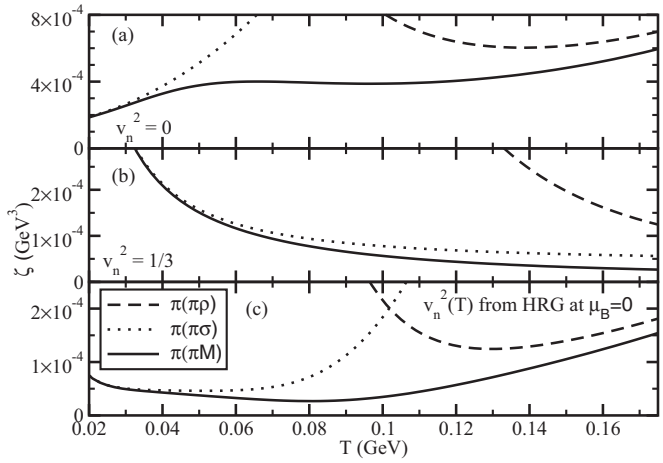

FIG. 3. $\zeta(T)$ due to pion thermal width for $\pi\sigma$ (dotted line), $\pi\rho$ (dashed line) loops, and their total (solid line) at $v_n^2 = 0$ (a), $v_n^2 = 1/3$ (b), and $v_n^2(T)$ from HRG (c). Blue circles represents the results of Ref. [37].

where n_l is BE distribution functions of π at energy $\omega_l = \{\vec{l}^2 + m_\pi^2\}^{1/2}$ and n_u^+ is FD distribution of B at energy $\omega_u = \{(\vec{k} - \vec{l})^2 + m_M^2\}^{1/2}$. With the help of the interaction Lagrangian densities from Eq. (17), the vertex factors $L_{N\pi B}(k,l)$ [48] have been obtained.

After the integration of the internal momentum $\vec{l}$, Eqs. (14), (16), and (18) will give the respective thermal width as a function of external momentum $\vec{k}$, T, and μ_B. With the help of Eqs. (12) and (13), the summation of different loop contributions will provide a detailed structure of Γ_π and Γ_N, which will have a nontrivial influence on the $\zeta(T,\mu_B)$. This is the main contribution which makes our studies different from the earlier HRG calculations of ζ [33–36].

III. RESULTS AND DISCUSSION

Let us start our numerical discussion with Fig. 2, where momentum dependence of thermal widths of pion and nucleon have been displayed. With the help of Eqs. (10), (11), (12), (14), and (16), Γ_π^M, Γ_π^B, and their total Γ_π can be found whose momentum dependence are, respectively, shown by dash-dotted, dotted and solid lines in Fig. 2. Similarly, Γ_N can be deduced by using Eqs. (18) and (13) and its momentum distribution is represented by dash line. Panels (a), (b), and (c) of Fig. 2 are for a different set of temperature T and baryon chemical potential μ_B of the medium. Though Γ_N is approximately constant with nucleon momentum, but Γ_π^M and Γ_π^B exhibit a peak structure in some point of the $\vec{k}$ axis, which depends on the medium parameters T and μ_B. These momentum distribution of Γ_π and Γ_N will be integrated out when we will estimate ζ_π and ζ_N from Eqs. (8) and (9), respectively.

Let us come to the different loop contributions of pion and nucleon thermal width in bulk viscosity coefficient of hadronic matter. Figure 3(c) shows individual contributions of $\pi\sigma$ (dotted line) and $\pi\rho$ (dash line) loops in ζ_π, which reveals that they are respectively important in low ($T < 0.080$ GeV) and high ($T > 0.080$ GeV) temperature domain for getting a nondivergent values of ζ_π. These are respectively obtained by putting $\Gamma_{\pi(\pi\sigma)}$ and $\Gamma_{\pi(\pi\rho)}$ in place of Γ_π of Eq. (8). Putting $\Gamma_\pi^M = \Gamma_{\pi(\pi\sigma)} + \Gamma_{\pi(\pi\rho)}$ in place of Γ_π of Eq. (8), we get the solid line, representing total bulk viscosity of pionic component due to meson loops. After a mild decrement in low T (<0.080 GeV), it receives an increment nature in high T (>0.080 GeV). We find good qualitative agreement with Ref. [37] shown by blue circles in Fig. 3(c). Along with Fig. 3(c), where an explicit temperature dependent v_n^2 is taken from HRG model, the results for $v_n^2 = 0$ and $v_n^2 = 1/3$ are also displayed in Figs. 3(a) and 3(b), which are little different in nature. Just to show the phase space sensitivity of bulk viscosity via v_n^2, these two results are displaying two extreme limits of v_n^2. Therefore, we can understand Fig. 3(c) as some sort of superposition of Figs. 3(a) and 3(b).

According to Eq. (12) different baryon loops contribution (Γ_π^B) should add with meson loops contribution (Γ_π^M) to give total pion thermal width Γ_π. In Fig. 4(a), changing the nature of dash-dotted line to dotted line indicates that inclusion of baryon loops with meson loops becomes the reason for reducing the rate of increment of $\zeta_\pi(T)$ at high temperature region, $T > 0.100$ GeV. Putting our calculated nucleon thermal width Γ_N in Eq. (9), we get ζ_N as shown by the dashed line in Fig. 4(a). Now adding ζ_N with ζ_π we have total bulk viscosity

$$\zeta_T = \zeta_\pi + \zeta_N, \tag{19}$$

as shown by solid line in Fig. 4(a). In Fig. 4(b), this ζ_T (solid line) has been compared with the results generated for two constant values of v_n^2 ($v_n^2 = 0.25$: dashed line and $v_n^2 = 0.15$: dotted line), within which $v_n^2(T,\mu_B = 0)$ from HRG model more or less varies.

At two different values of μ_B, $\zeta(T)$ due to nucleon thermal width (Γ_N), pion thermal width for meson loops (Γ_π^M), and meson + baryon loops (Γ_π) are shown in Figs. 5(a), 5(b),

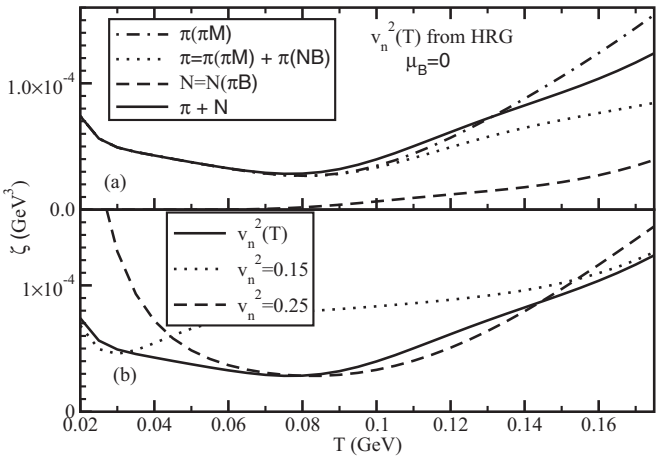

FIG. 4. (a) Temperature dependence of bulk viscosity for pion thermal width with mesonic loops (dash-dotted line), meson + baryon loops (dotted line), for nucleon thermal width (dashed line), and their total $\zeta_T = \zeta_\pi + \zeta_N$ (solid line). (b) $\zeta(T)$ for $v_n^2(T)$ from HRG and two constant values of v_n^2 ($v_n^2 = 0.15$: dotted line and $v_n^2 = 0.25$: dashed line).

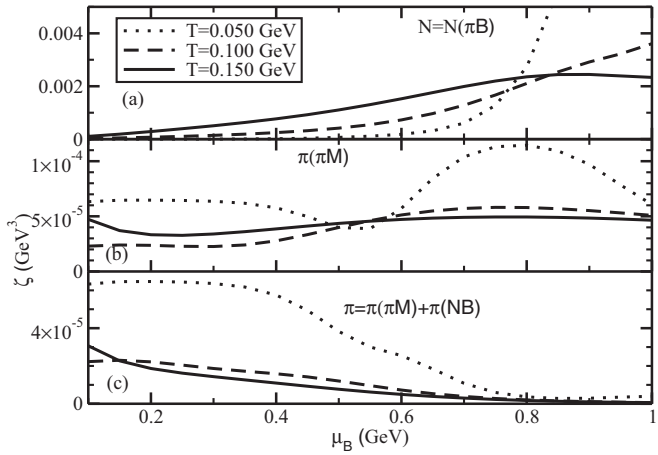

FIG. 6. Same as Fig. 5 along μ_B axis at $T = 0.050$ GeV (dotted line), 0.100 GeV (dashed, line) and 0.150 GeV (solid line).

and 5(c) respectively. Similarly, Figs. 6(a), 6(b), and 6(c) displays different loop contributions in $\zeta(\mu_B)$ at $T = 0.050$ GeV (dotted line), 0.100 GeV (dashed line), and 0.150 GeV (solid line). From Figs. 5(a) and 6(a), we see that ζ_N increases with T as well as μ_B. From Fig. 5(b), we see the ζ_π due to Γ_π^M at finite μ_B first decreases at low T then increases at high T. The nature of these curves is quite similar to the curve of $\zeta_\pi(T)$ at vanishing μ_B but their minima are only shifted towards lower T as μ_B increases. Following the same story of vanishing μ_B, the inclusion of baryon loops in pion self-energy is again influencing $\zeta_\pi(T)$ in the high temperature domain. The variations with μ_B of $\zeta_N(\mu_B)$ in Fig. 6(a) and $\zeta_\pi(\mu_B)$ in Fig. 6(b) and 6(c) are grossly the same as their temperature dependence. For small T and μ_B, ζ_N and ζ_π are of similar order. However, with increasing T and μ_B, ζ_N dominates over ζ_π. ζ_N receives additional contribution from $(\frac{\partial P}{\partial n_B})_\epsilon$. One should keep in mind that the term $(\frac{\partial P}{\partial n_B})_\epsilon$ goes to zero for $\mu_B = 0$. The T and μ_B dependence of $(\frac{\partial P}{\partial n_B})_\epsilon$ are shown in Figs. 7(b) and 7(d), respectively, while Figs. 7(a) and 7(c) displays the T and μ_B dependence of v_n^2. From Fig. 7(a), we see that our $v_n^2(T, \mu_B = 0)$ curve (solid line) is in good agreement with LQCD results [3] (circles) within the hadronic temperature domain ($T < 0.160$ GeV). Total bulk viscosity ζ_T (a), entropy density s (b), and their ratio ζ/s (c) are plotted against T in Fig. 8 and μ_B in Fig. 9 at three different values μ_B and T, respectively. Since the increment of $s(T)$ is larger than the increment of $\zeta(T)$, therefore, ζ/s appears as a decreasing function of T. On the other hand, both $\zeta(\mu_B)$ and $s(\mu_B)$ monotonically increase with μ_B but the ratio $\zeta/s(\mu_B)$ increases first and then decreases at a high μ_B domain. Next,

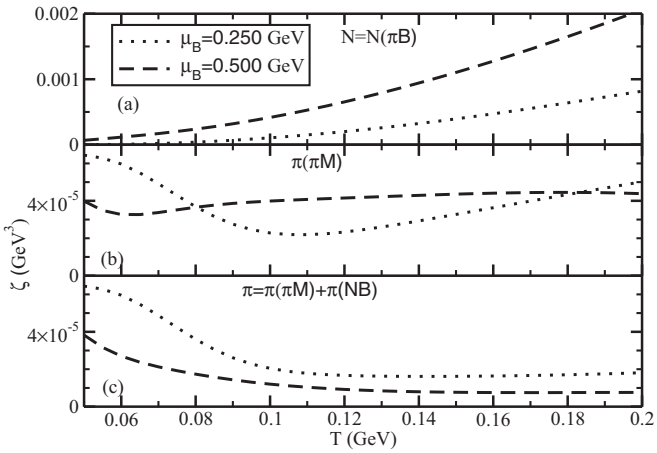

FIG. 5. $\zeta(T)$ due to nucleon thermal width (a), pion thermal width for meson loops (b), and meson + baryon loops (c) at $\mu_B = 0.250$ GeV (dotted line) and 0.500 GeV (dashed line).

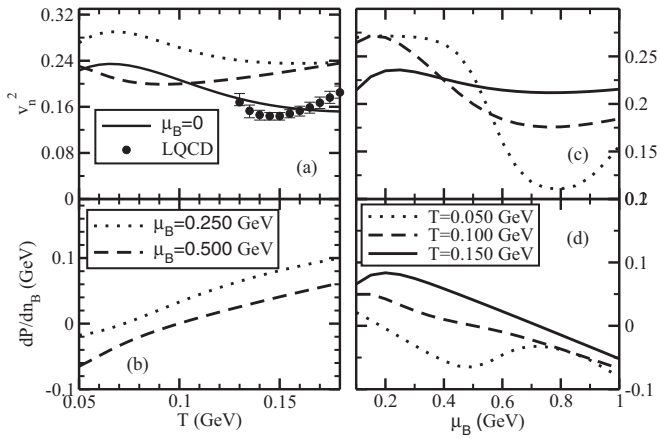

FIG. 7. (a) $v_n^2(T)$ at $\mu_B = 0$ (solid line), 0.250 GeV (dotted line), and 0.500 GeV (dashed line), and LQCD results of $v_n^2(T, \mu_B = 0)$ (circles) [3]; (b) $(\frac{\partial P}{\partial n_B})_\epsilon$ vs T at $\mu_B = 0.250$ GeV (dotted line) and 0.500 GeV (dashed line); (c) $v_n^2(\mu_B)$ at $T = 0.050$ GeV (dotted line), 0.100 GeV (dashed line), and 0.150 GeV (solid line); (d) $(\frac{\partial P}{\partial n_B})_\epsilon$ vs μ_B at $T = 0.050$ GeV (dotted line), 0.100 GeV (dashed line), and 0.150 GeV (solid line).

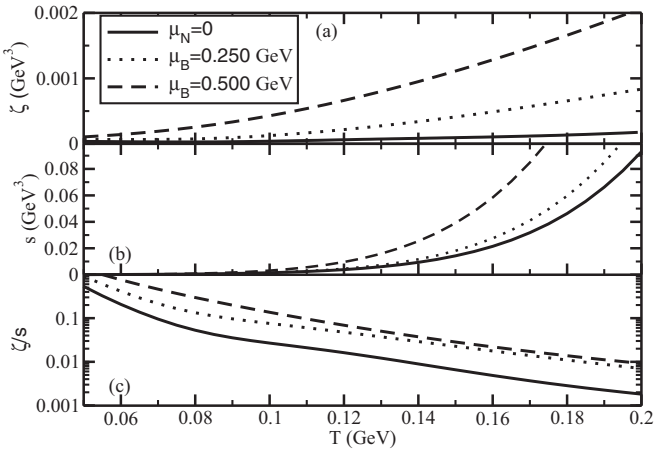

FIG. 8. T dependence of total bulk viscosities (a), entropy densities from HRG (b), and their ratios ζ/s (c) at $\mu_B = 0$ (solid line), 0.250 GeV (dotted line) and 0.500 GeV (dashed line).

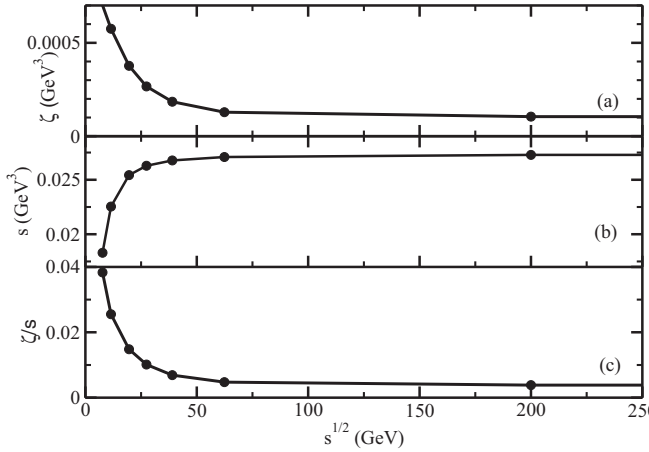

FIG. 10. Center of mass energy ($\sqrt{s}$) dependence of total bulk viscosity (a), entropy density from HRG (b), and their ratio ζ/s (c).

Figs. 10(a), 10(b), and 10(c) reveals, respectively, the variation of total bulk viscosity ζ, entropy density s, and their ratio with the variation of center of mass energy $\sqrt{s}$. (The reader is requested to be careful of the same symbol s, used for entropy density and square of beam energy.) The beam energy dependence of T and μ_B used in computation are those obtained from fits to hadron yields. We have used the parametrization from Ref. [50]. We notice in Fig. 10 that ζ (a) as well as ζ/s (c) decrease with $\sqrt{s}$, which is qualitatively agreeing with the results of earlier studies [33,34]. The decreasing trend of ζ and ζ/s with $\sqrt{s}$ can be understood from the fact that μ_B decreases with $\sqrt{s}$ while T remains fairly constant in the range of $\sqrt{s}$ analyzed here and according to Figs. 9(a) and 9(c), the ζ and ζ/s decrease with decreasing of μ_B.

Figure 11 is dedicated to a comparative understanding of our results with respect to the earlier investigations. As most of the works have been done at $\mu_B = 0$, so we have plotted ζ (a) and ζ/s (b) against T for $\mu_B = 0$, which are compared with the results, obtained by Sasaki *et al.* (green triangles down [20]), Deb *et al.* (pink solid squares [25]), Chakraborty *et al.* (brown stars [28]), Marty *et al.* (open circles [21]), Kadam *et al.* (violet pluses [34]), Fraile *et al.* (blue solid circles [37]), Hostler *et al.* (open squares [36]), Mitra *et al.* (grey triangles up [32]). We have presented our results for π component, $(\pi + N)$ components and $(\pi + N +$ other resonances $R)$ components by dotted, dashed, and solid lines, respectively. We see a large numerical band for ζ (10^{-5}–10^{-2} GeV^3) or ζ/s (10^{-3}–10^{0}), within which earlier estimations are located. Most of the earlier works [20,21,25,27,28,32,34–37] based on effective QCD model calculations [20,21,25,27,28] as well as effective hadronic model calculations [32,34–37] predicted a decreasing function of $\zeta/s(T)$ in the hadronic temperature domain, which is qualitatively similar with our results. These

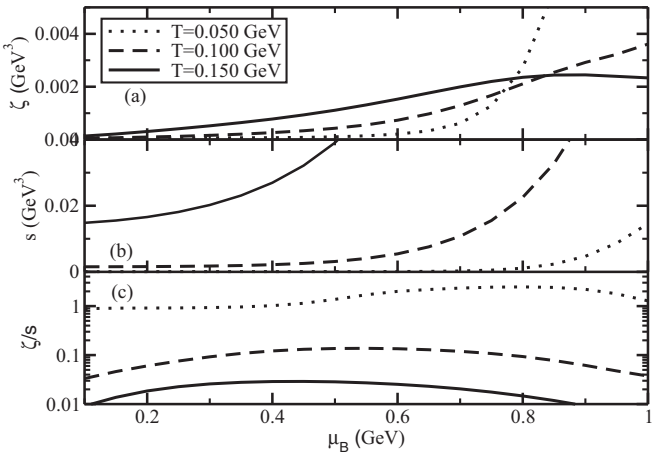

FIG. 9. μ_B dependence of total bulk viscosities (a), entropy densities from HRG (b), and their ratios ζ/s (c) at $T = 0.050$ GeV (dotted line), 0.100 GeV (dashed line), and 0.150 GeV (solid line).

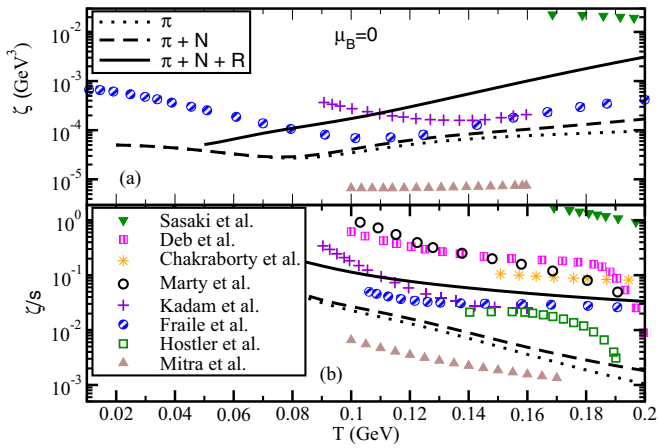

FIG. 11. Our results of ζ (a) and ζ/s (b) vs T at $\mu_B = 0$ for π component (dotted line), $(\pi + N)$ components (dashed line) and $(\pi + N +$ other resonances $R)$ components are compared with the earlier results of Sasaki *et al.* (green triangles down [20]), Deb *et al.* (pink solid squares [25]), Chakraborty *et al.* (brown stars [28]), Marty *et al.* (open circles [21]), Kadam *et al.* (violet pluses [34]), Fraile *et al.* (blue solid circles [37]), Hostler *et al.* (open squares [36]), Mitra *et al.* (grey triangles up [32]).

do not support the fact that ζ/s diverges or becomes large near the transition temperature as indicated by Refs. [2,4,5], within the temperature domain of the quark phase. Some of the effective QCD model calculations [22–24,27], which can predict estimations of ζ/s in both temperature domains, exposed a peak structure near the transition temperature.

For quantitative comparison, the results of other HRG model calculations [33–36] may be more meaningful to focus on rather than other microscopic calculations. Among them [33–36], only Ref. [34] has taken the RTA expression of ζ like us but Refs. [33,36] have taken the Kubo-type expression of ζ in the QCD sum rule approach [2,5]. Hence, Ref. [34] may be the best one to compare. While Ref. [34] uses (approximately) constant values of relaxation time for all hadrons, our ζ is constructed by the momentum dependent relaxation time of pion and nucleon. In order to treat our results in equal footing with Ref. [34], we have added the contributions of other resonances by taking our thermal width of pion and nucleon for other mesons and baryons, respectively. By this way, the total contribution of ζ and ζ/s, as shown by solid lines in Figs. 11(a) and 11(b), respectively, are approximately (in order of magnitude) close to the results of Ref. [34], shown by violet pluses. The main contributing ingredient of our work is using the explicit structure of momentum and temperature dependent thermal width or relaxation time of hadrons assuming an underlying model for the interaction dynamics, instead of their (approximately) constant values, adopted in Ref. [34]. This quantitatively modifies the numerical values of ζ and ζ/s (solid lines) with respect to those of Ref. [34] (violet pluses).

Taking shear viscosity $\eta(T,\mu_B = 0)$ from Ref. [47], based on same pion and nucleon thermal fluctuations, we get $\zeta/\{(1/3 - v_n^2)^2\eta\} \approx 5 - 4$ and $\zeta/\{(1/3 - v_n^2)\eta\} \approx 0.8 - 0.7$. This supports the estimation of gravity dual theory [51] instead of the relation $\zeta/\{(1/3 - v_n^2)^2\eta\} \approx 15$, followed by photon fields [52], scalar fields [53], or QCD theory [19]. So our estimation within the hadronic temperature domain represents the strongly coupled picture instead of weakly coupled scenario [19].

IV. SUMMARY

We have gone through a detailed microscopic calculation of the bulk viscosity coefficient for hadronic matter, where thermodynamical equilibrium conditions of all hadrons in medium have been treated by the standard HRG model, which is very successful to generate LQCD thermodynamics up to the transition temperature. The thermal widths of medium constituents in the bulk viscosity expressions inversely determine their numerical strengths. Assuming pions and nucleons as the most abundant medium constituents, we have concentrated on the bulk viscosity contributions from pion and nucleon components, where their corresponding thermal widths are derived from their in-medium scattering probabilities with different mesonic and baryonic resonances in the hadronic matter. Owing to the field theory version of the optical theorem, the imaginary part of pion and nucleon self-energies (on-shell) at finite temperature give the estimation of their corresponding thermal widths. In the one-loop diagrams of pion self-energy, we have taken different mesonic and baryonic loops, while pion-baryon intermediate states are considered in the one-loop diagrams of nucleon self-energy. Their thermal widths are basically on-shell values of their corresponding Landau cut contributions, which disappear in the absence of medium and therefore, these are inversely interpreted as their respective relaxation times, which proportionally control the numerical strength of ζ. Our results show that $\zeta(T)$ at $\mu_B = 0$ increases in the high temperature domain $[0.080 < T(\text{GeV}) < 0.175]$ but a decreasing nature of $\zeta(T)$ has also been observed at low T (< 0.08 GeV). The $\pi\sigma$ and $\pi\rho$ loops of pion self-energy are respectively responsible for the decreasing and increasing nature of $\zeta(T)$ at low and high T domains. The addition of baryon loops in pion self-energy mainly make $\zeta(T)$ reduce at the high T domain. Bulk viscosity for the nucleon component monotonically increases with T. At finite μ_B, the nucleon component of bulk viscosity is highly dominant over the pion component. Adding nucleon and pion components, the total ζ increases with both T and μ_B. However, after dividing by total entropy density, ζ/s appear as a decreasing function of T and with the variation of μ_B, it increases first at the low μ_B region and then decreases at the high μ_B region. Along the beam energy axis, the ζ and ζ/s both decrease, as noticed in some earlier works [33–35].

During a comparison with theearlier results of $\zeta/s(T)$ at $\mu_B = 0$, one can notice that the qualitative as well as quantitative nature is not a very settled issue. Some of them [2,4,5] indicated a divergence tendency of ζ/s near transition temperature, some effective QCD model calculations [22–24,27] revealed a peak structure near transition temperature, whereas most of the effective QCD model calculations [20,21,25,27,28] as well as effective hadronic model calculations [32,34–37], including our present work, predict a decreasing function of $\zeta/s(T)$ in the hadronic temperature domain, with a few exceptional HRG calculations [33,36]. From the relation between shear [47] and bulk viscosities, having the same dynamical origin, a strongly coupled picture of hadronic matter is revealed by this present work.

ACKNOWLEDGMENTS

During the first and major part of this work, S.G. was financially supported by the DST project no. NISER/R&D-34/DST/PH1002, (with title "Study of QCD phase Structure through high energy heavy ion collisions" and principal investigator Prof. B. Mohanty). During the last part of the work, S.G. was supported from UGC Dr. D. S. Kothari Post Doctoral grant no. F.4-2/2006 (BSR)/PH/15-16/0060. S.C. acknowledges XIIth plan project no. 12-R&D-NIS-5.11-0300 and CNT project PIC XII-R&D-VECC-5.02.0500 for support. S.G. thanks the high energy group of NISER (Prof. B. Mohanty, Dr. A. Das, Dr. C. Jena, Dr. R. Singh, R. Haque, V. Bairathi, K. Nayak, V. Lyer, S. Kundu, and others) and group of Calcutta University (Prof. A. Bhattacharyya, Prof. G. Gangopadhyay) for getting various academic and nonacademic support at NISER and CU during this work and also thanks Dr. V. Roy and Prof. H. Mishra for some discussion regarding this work.

[1] P. K. Kovtun, D. T. Son, and A. O. Starinets, Phys. Rev. Lett. **94**, 111601 (2005).
[2] D. Kharzeev and K. Tuchin, J. High Energy Phys. 09 (2008) 093.
[3] A. Bazavov *et al.* (HotQCD Collaboration), Phys. Rev. D **90**, 094503 (2014).
[4] H. B. Meyer, Phys. Rev. Lett. **100**, 162001 (2008)
[5] F. Karsch, D. Kharzeev, and K. Tuchin, Phys. Lett. B **663**, 217 (2008).
[6] G. Torrieri and I. Mishustin, Phys. Rev. C **78**, 021901(R) (2008).
[7] A. Monnai and T. Hirano, Phys. Rev. C **80**, 054906 (2009).
[8] G. S. Denicol, T. Kodama, T. Koide, and P. Mota, Phys. Rev. C **80**, 064901 (2009).
[9] K. Rajagopal and N. Tripuraneni, J. High Energy Phys. 03 (2010) 018.
[10] P. Bozek, Phys. Rev. C **81**, 034909 (2010); **85**, 034901 (2012); P. Bozek and I. Wyskiel-Piekarska, *ibid.* **85**, 064915 (2012).
[11] H. Song and U. W. Heinz, Phys. Rev. C **81**, 024905 (2010).
[12] J. Bhatt, H. Mishra, and V. Sreekanth, J. High Energy Phys. 11 (2010) 106; Phys. Lett. B **704**, 486 (2011); Nucl. Phys. A **875**, 181 (2012).
[13] K. Dusling and T. Schäfer, Phys. Rev. C **85**, 044909 (2012).
[14] V. Roy and A. K. Chaudhuri, Phys. Rev. C **85**, 024909 (2012).
[15] J. Noronha-Hostler, G. S. Denicol, J. Noronha, R. P. G. Andrade, and F. Grassi, Phys. Rev. C **88**, 044916 (2013).
[16] J. Noronha-Hostler, J. Noronha, and F. Grassi, Phys. Rev. C **90**, 034907 (2014).
[17] M. Habich and P. Romatschke, J. High Energy Phys. 12 (2014) 054.
[18] S. Ryu, J. F. Paquet, C. Shen, G. S. Denicol, B. Schenke, S. Jeon, and C. Gale, Phys. Rev. Lett. **115**, 132301 (2015).
[19] P. Arnold, C. Dogan, and G. D. Moore, Phys. Rev. D **74**, 085021 (2006).
[20] C. Sasaki and K. Redlich, Phys. Rev. C **79**, 055207 (2009); Nucl. Phys. A **832**, 62 (2010).
[21] R. Marty, E. Bratkovskaya, W. Cassing, J. Aichelin, and H. Berrehrah, Phys. Rev. C **88**, 045204 (2013).
[22] S. Xiao, L. Zhang, P. Guo, and D. Hou, Chin. Phys. C **38**, 054101 (2014).
[23] S. Ghosh, T. C. Peixoto, V. Roy, F. E. Serna, and G. Krein, Phys. Rev. C **93**, 045205 (2016).
[24] K. Saha and S. Upadhaya, arXiv:1505.00177 [hep-ph].
[25] P. Deb, G. P. Kadam, and H. Mishra, arXiv:1603.01952 [hep-ph].
[26] K. Paech and S. Pratt, Phys. Rev. C **74**, 014901 (2006).
[27] A. Dobado and J. M. Torres-Rincon, Phys. Rev. D **86**, 074021 (2012); A. Dobado, F. J. Llanes-Estrada, and J. Torres Rincon, Phys. Lett. B **702**, 43 (2011).
[28] P. Chakraborty and J. I. Kapusta, Phys. Rev. C **83**, 014906 (2011).
[29] V. Chandra, Phys. Rev. D **84**, 094025 (2011); **86**, 114008 (2012).
[30] S. K. Das and Jan-e Alam, Phys. Rev. D **83**, 114011 (2011).
[31] S. Gavin, Nucl. Phys. A **435**, 826 (1985).
[32] S. Mitra and S. Sarkar, Phys. Rev. D **87**, 094026 (2013); S. Mitra, U. Gangopadhyaya, and S. Sarkar, *ibid.* **91**, 094012 (2015).
[33] G. P. Kadam and H. Mishra, Nucl. Phys. A **934**, 133 (2014).
[34] G. P. Kadam and H. Mishra, Phys. Rev. C **92**, 035203 (2015); **93**, 025205 (2016).
[35] G. Sarwar, S. Chatterjee, and J. Alam, arXiv:1512.06496 [nucl-th].
[36] J. Noronha-Hostler, J. Noronha, and C. Greiner, Phys. Rev. Lett. **103**, 172302 (2009).
[37] D. Fernandez-Fraile and A. Gomez Nicola, Eur. Phys. J. C **62**, 37 (2009); Phys. Rev. Lett. **102**, 121601 (2009).
[38] A. Wiranata and M. Prakash, Nucl. Phys. A **830**, 219c (2009); M. Prakash, M. Prakash, R. Venugopalan, and G. Welke, Phys. Rep. **227**, 321 (1993).
[39] K. A. Olive *et al.* (Particle Data Group), Chin. Phys. C **38**, 090001 (2014).
[40] A. Bazavov, T. Bhattacharya, M. Cheng *et al.*, Phys. Rev. D **80**, 014504 (2009).
[41] S. Borsanyi *et al.*, J. High Energy Phys. 09 (2010) 073.
[42] S. Borsanyi, Z. Fodor, S. D. Katz, S. Krieg, C. Ratti, and K. Szabo, J. High Energy Phys. 01 (2012) 138.
[43] M. Albright and J. I. Kapusta, Phys. Rev. C **93**, 014903 (2016).
[44] S. Ghosh, G. Krein, and S. Sarkar, Phys. Rev. C **89**, 045201 (2014).
[45] M. Post, S. Leupold, and U. Mosel, Nucl. Phys. A **741**, 81 (2004).
[46] S. Ghosh, J. Phys. G **41**, 095102 (2014).
[47] S. Ghosh, Braz. J. Phys. **45**, 687 (2015).
[48] S. Ghosh, Phys. Rev. C **90**, 025202 (2014).
[49] S. Ghosh, Braz. J. Phys. **44**, 789 (2014).
[50] F. Karsch and K. Redlich, Phys. Lett. B **695**, 136 (2011)
[51] P. Benincasa, A. Buchel, and A. O. Starinets, Nucl. Phys. B **733**, 160 (2006); A. Buchel, Phys. Rev. D **72**, 106002 (2005).
[52] S. Weinberg, Astrophys. J. **168**, 175 (1971).
[53] R. Horsley and W. Schoenmaker, Nucl. Phys. B **280**, 716 (1987).